

DIGITAL CONTROL OF CONICAL MOTION OF HIGH SPEED ROTORS SUSPENDED BY MAGNETIC BEARINGS IN CASE OF LARGE SAMPLING PERIOD

Chikara MURAKAMI

Tokyo Metropolitan Institute of Technology,
6-6, Asahigaoka, Hino-shi, Tokyo 191, JAPAN

ABSTRACT

In this paper, digital control of exclusively two conical modes of rigid spinning rotor is treated. If, sampling period $T > T_n$ where T_n is nutation or high speed mode (N-mode) period, it is apparent that suppression of that mode becomes difficult.

Control strategy is to move low speed mode (P-mode) component of angular momentum vector H of the rotor towards central axis position for P-mode suppression, and N-mode component of H towards the spinning axis for N-mode suppression. In case of $T > T_n$, more sophisticated control law is required. A detailed analysis is given. Several simulation examples including the cases of $T > T_n$ are given showing effectiveness of proposed control law.

1. INTRODUCTION

Digital signal processors (DSPs) are more and more advancing and becoming cheaper. However, to make sampling period including, for example, observer computation small is one of remained difficult problems. If, an advanced software which can suppress two conical modes even in case of $T > T_n$ appeared, many analog control circuits will be replaced by DSPs.

Another problem in digital control is the fact that negative restoring or

spring constants to deviation of the rotor which is generated by bias magnetic flux for linearization, is unavoidable.

However, cylindrical or translational motion is rather simple and has no resonance in case of negative spring constants. Therefore, translational motion is not treated in this paper.

At first, discrete systems with zero-order-hold of a controlled model is given using complex number variables on the assumption that tilting angle of the rotor θ and its rate signal $\dot{\theta}$ are available. Then, solution of two free modes after the end of control torque U are given. The solution is used for finding optimal directions of U for suppression of each mode.

2. CONTROLLED MODEL

Direction of momentum vector, H , of an axi-symmetric rotor viewed from Z-axis of inertia coordinate, X-Y-Z, is easily obtained from tilting angle, θ , of the rotor axis vector S and its rate signal, $\dot{\theta}$ which are supposed to be available for control. Direction angles of the two vectors, S and H , from Z-axis are small and can be described by complex numbers \underline{S} and \underline{H} on a complex number plane (see Fig.1, underlined letters mean complex numbers), or, they are expressed as

$$\underline{S} = S_x + jS_y = \theta_x \hat{x} - j\theta_y \hat{y} = -j\theta \quad (1)$$

$$\underline{H} = \underline{S} + Id(\dot{\theta}_x + j\dot{\theta}_y) / |H| \quad (2)$$

where θ_x and θ_y are tilting angle of S about X - and Y -axis, respectively, j is complex number unit and Id is radial moment of inertia of the rotor. Using

$$\underline{\dot{\theta}} = \dot{\theta}_x \hat{x} + j\dot{\theta}_y \hat{y} \quad (3)$$

$$h = |H| / Id = Ip\omega / Id = \sigma \omega \quad (4)$$

$$\sigma = Ip / Id \quad (5)$$

where Ip is polar moment of inertia, and ω is rotation velocity of the rotor, nutation angle N is expressed as

$$\underline{N} = \underline{H} - \underline{S} = \underline{\dot{\theta}} / h \quad (6)$$

Using these notations and control torque as shown

$$\underline{U}(kT) = U_x(kT) + jU_y(kT) \quad (7)$$

equation of motion is expressed as

$$Id \underline{\ddot{\theta}} - jH \underline{\dot{\theta}} - K \underline{\theta} = \underline{U}(kT), \quad (k=0, 1, 2, \dots) \quad (8)$$

where K is unstable spring constant due to bias flux.

Dividing Eq. (8) by Id , omitting T , and using small letters: e.g. $H/Id \rightarrow h$, we get

$$\underline{\ddot{\theta}} - jh \underline{\dot{\theta}} - k \underline{\theta} = \underline{u}(k), \quad (k=0, 1, 2, \dots) \quad (9)$$

If, we use state variable $x = [\underline{\theta}, \underline{\dot{\theta}}]^T$ and output $y = [\underline{S}, \underline{N}]^T$, conventional state equation and output equation are

$$\dot{x} = Ax + bu$$

$$y = Cx$$

where

$$A = \begin{bmatrix} 0 & 1 \\ k & jh \end{bmatrix}, \quad b = \begin{bmatrix} 0 \\ 1 \end{bmatrix}, \quad C = \begin{bmatrix} -i & 0 \\ 0 & 1/h \end{bmatrix} \quad (10)$$

Using transition matrix $\Phi(t)$, we can get the following discrete systems:

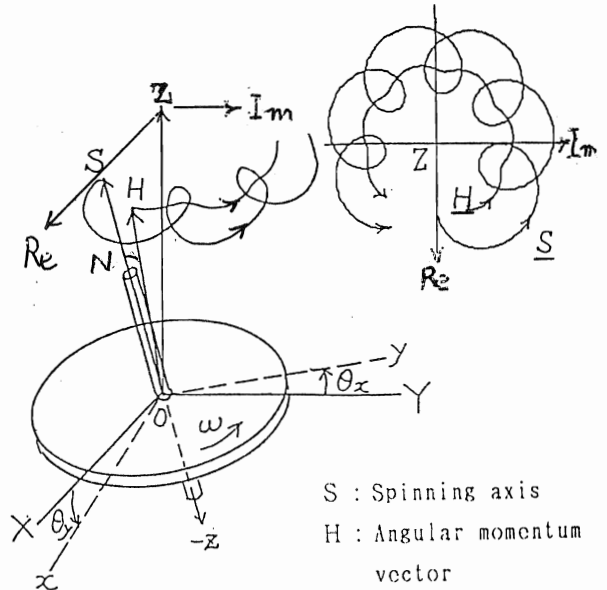


FIGURE 1 : Coordinate System

$$\begin{bmatrix} \underline{S}(k+1) \\ \underline{N}(k+1) \end{bmatrix}^T = \Phi(T) \begin{bmatrix} \underline{S}(k) \\ \underline{N}(k) \end{bmatrix}^T + \int_0^T \Phi(T-\eta) \begin{bmatrix} -j\phi_{12}(\eta) \\ \phi_{22}(\eta) \end{bmatrix} / H^T d\eta \underline{U}(k) \quad (11)$$

$$\text{where } \Phi(t) = \begin{bmatrix} \phi_{11}(t) & \phi_{12}(t) \\ \phi_{21}(t) & \phi_{22}(t) \end{bmatrix} \quad (12)$$

$$\phi_{11}(t) = \langle (\lambda_n - h) \exp[j\lambda_n t] + (h - \lambda_p) \exp[j\lambda_p t] \rangle / (\lambda_n - \lambda_p) \quad (13)$$

$$\phi_{12}(t) = j \langle -\exp[j\lambda_n t] + \exp[j\lambda_p t] \rangle / (\lambda_n - \lambda_p) \quad (14)$$

$$\phi_{21}(t) = k \phi_{12}(t) \quad (15)$$

$$\phi_{22}(t) = \langle \lambda_n \exp[j\lambda_n t] - \lambda_p \exp[j\lambda_p t] \rangle / (\lambda_n - \lambda_p) \quad (16)$$

The second or integration term of right-hand side of Eq. (11) expressed by

$$q(T) \underline{U}(k) = [q_1(T), q_2(T)]^T \underline{U}(k) \quad (17)$$

becomes after integration as follows:

$$q_1(T) = j \langle (1 - \exp[\lambda_p T]) / \lambda_p \rangle - \langle (1 - \exp[\lambda_n T]) / \lambda_n T \rangle / (\lambda_n - \lambda_p) \quad (18)$$

$$q_2(T) = j \langle \exp[\lambda_p T] - \exp[\lambda_n T] \rangle / \langle (\lambda_n - \lambda_p) H \rangle \quad (19)$$

1. FREE MOTION AFTER EXCITATION

Discrete form of output $y(t)$ is

$$y(k+1) = \Phi(T)y(k) + q\underline{U}(k) \quad (20)$$

output $y([k+1]T+t)$ of free motion after the end the following one rectangular \underline{U} :

$$\underline{U}(k) = \begin{cases} \underline{U} & k=1 \\ 0 & k \geq 2 \end{cases} \quad (21)$$

is now required for determination of $\underline{U}(k+1)$. We can get it easily:

$$y(t) = \Phi(t) [\Phi(T)y(k) + q\underline{U}] \quad (22)$$

After some manipulations, coefficients of $\exp[j\lambda_n t]$ and $\exp[j\lambda_p t]$ of $\underline{S}(t)$ in $y(t)$, \underline{S}_n and \underline{S}_p , respectively, are given as follows:

$$\underline{S}_n = -[\lambda_p \underline{S}(k) + h\underline{N}(k) + j(\underline{U}/\lambda_n)(1 - \exp[j\lambda_n T])] / (\lambda_n - \lambda_p) \quad (23)$$

$$\underline{S}_p = [\lambda_n \underline{S}(k) + h\underline{N}(k) + j(\underline{U}/\lambda_p)(1 - \exp[j\lambda_p T])] / (\lambda_n - \lambda_p) \quad (24)$$

Equations (23) and (24) express amplitudes of each mode after excitation of one rectangular torque \underline{U} . Therefore, \underline{U} must be determined so as to decrease both \underline{S}_n and \underline{S}_p .

4. DETERMINATION OF \underline{U}

Equations (23) and (24) are similar forms each other and expressed as

$$\underline{S}_c = A_c \langle \underline{B}_c + j\underline{U}K_c(1 - \exp[j\lambda_c T]) \rangle \quad (25)$$

where A_c, B_c and K_c are constants including initial values, and $c=n$ or p . In Eq.(25), the second term inside of $\langle \rangle$ is a chord of a circle whose radius is $\underline{U}K_c$ as shown in Fig.2. This chord, \underline{U}_c , has an advanced angle, $\lambda_c T/2$, to \underline{U} . To make \underline{S}_c small, direction of \underline{U}_c should coincide with direction of $-\underline{B}_c$, i.e. direction of \underline{U} should be behind to \underline{B}_c by $\lambda_c T/2$.

Chord length $U_c = |\underline{U}_c|$ is an effective

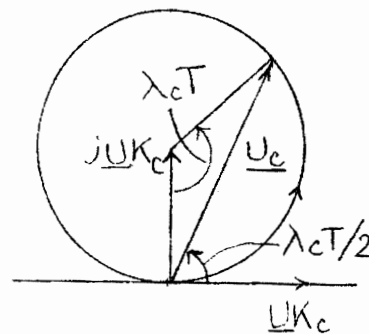


FIGURE 2 : Explanation of Eq.(25)

magnitude of \underline{U} which depends on sampling period T .

Note that

if T coincide with mode period, \underline{U}_c becomes zero, and the mode is uncontrollable.

If T is near to the mode period, U_c becomes small.

Rearranging Eq.(25), an important formula is derived:

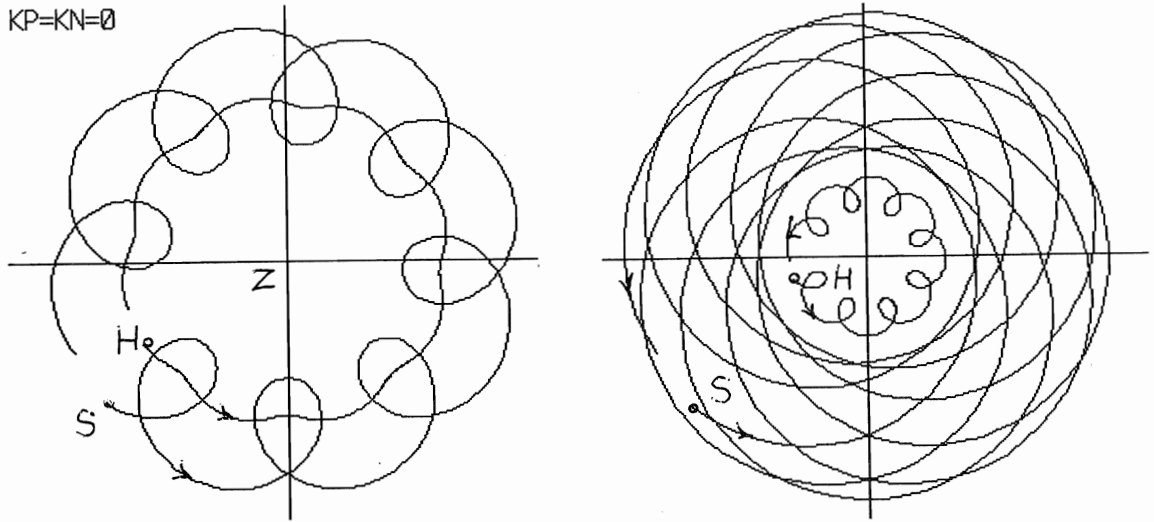
$$\underline{B}_c + K_c \underline{U} 2 \sin[\lambda_c T/2] \exp[j\lambda_c T/2] = 0 \quad (26)$$

From Eq.(26), we can get a feedback torque $K_c \underline{U}$ which completely vanish the mode:

$$K_c \underline{U} = -\underline{B}_c \exp[-j\lambda_c T/2] / (2 \sin[\lambda_c T/2]) \quad (27)$$

where K_c is feedback gain.

Unfortunately, it is rare that $K_p \underline{U}$ and $K_n \underline{U}$ coincide each other. Therefore, Eq.(27) should be used for determination of direction only. One half magnitude of Eq.(27) may be one good standard.



(a) Large P- and Small N-mode

(b) Large N- and Small P-mode

FIGURE 3 : Free Motion with Large P-mode and N-mode

5. SIMULATION EXAMPLES

A simulated model is

$\omega = 2000$ [rad/s] = 19,108 [rpm], angular velocity, and eigen values are:
 $\lambda_p = 88.2$ [rad/s] (period $T_p = 71$ [ms]),
 $\lambda_n = 918$ [rad/s] (period $T_n = 6.84$ [ms]),
 σ (moment of inertia ratio) = 0.5.

In the following, although several T is used, gain K_n and K_p are equal and set to a fixed values determined at small T . Sometimes $K_p = 0$ is tried to see effects of K_n on P-mode. Only loci of \underline{S} and \underline{H} will be shown. Simulation time is 62 [ms] if no notes.

At first, the case of control $\underline{U} = 0$ with two different initial conditions are shown in Fig.3, where no convergence or divergence is observed, showing correct numerical integration.

Figure 4 is three cases of $T < T_n$. The longer T , the larger effects on P-mode are seen. Especially, in $T = 0.9T_n$ case, locus of \underline{H} becomes distorted spiral.

Figure 5 is two cases of $T = 1.81T_n$, whose initial conditions are the same as Fig.3. Damping becomes worse compared to the last case of Fig.4.

Figure 6 is a case of $T = 2.27T_n$, where initially P-mode diverges a little as N-mode decays relatively quickly. About 200ms after, P-mode begins to converge slowly, as shown in the lower part.

6. DISCUSSION

If, $T \ll T_n$, it seems possible to suppress either mode separately. If, we move total \underline{H} towards \underline{S} , then \underline{H} moves outside, leading to P-mode divergence. Therefore, mode separation control was very effective, at least $T \ll T_n$.

In this paper, maximum T in presented simulation example is 15.5 [ms] = 2.27 T_n . The author has tried 31.1 [ms] = 4.54 T_n . The result was success. However, initial response was divergence of P-mode just as Fig.6, and it required long time that by far week convergece began.

Therefore, $T > 2T_n$ is theoretically possible, but not practical.

Another possibility is, for example in case of $2T_n < T < 3T_n$, $\underline{U} = 0$ for $t < 2T$, control begin at $t = 2T_n$. One cycle of \underline{U} in Fig.2 is useless for N-mode, moreover may be harmful for P-mode. It would be worthwhile researching this problem.

7. Concluding Remarks

Using transition matrix with complex number variables, analytical solution for mode separation control was given. Usefulness of optimal direction of control torque based on the analytical solution were proved using many simulation examples.

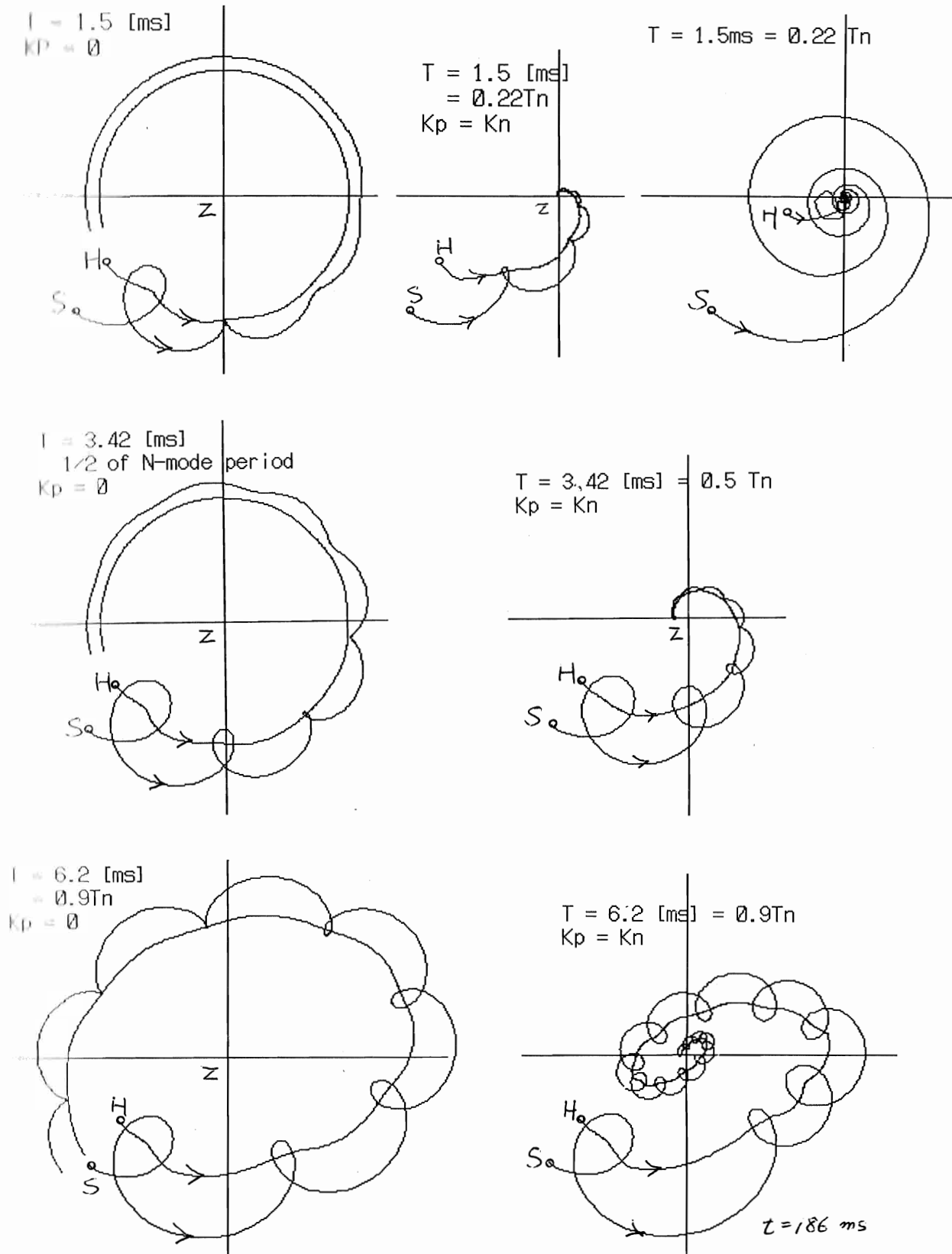


FIGURE 4 : Simulation of $T < T_n$ Three Cases with Various Control

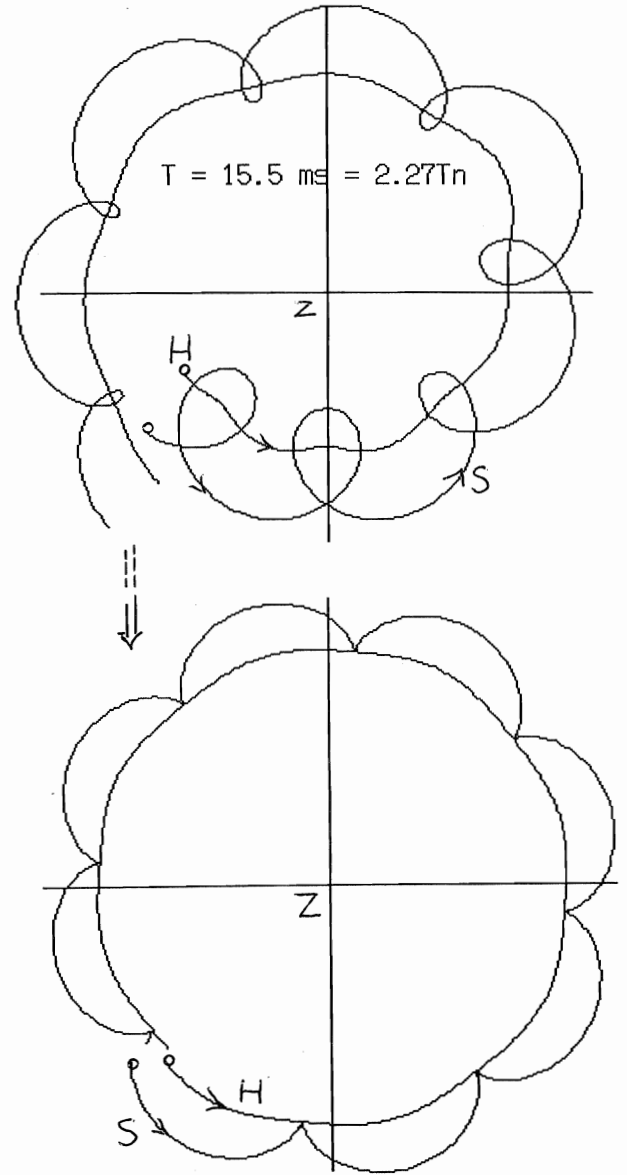
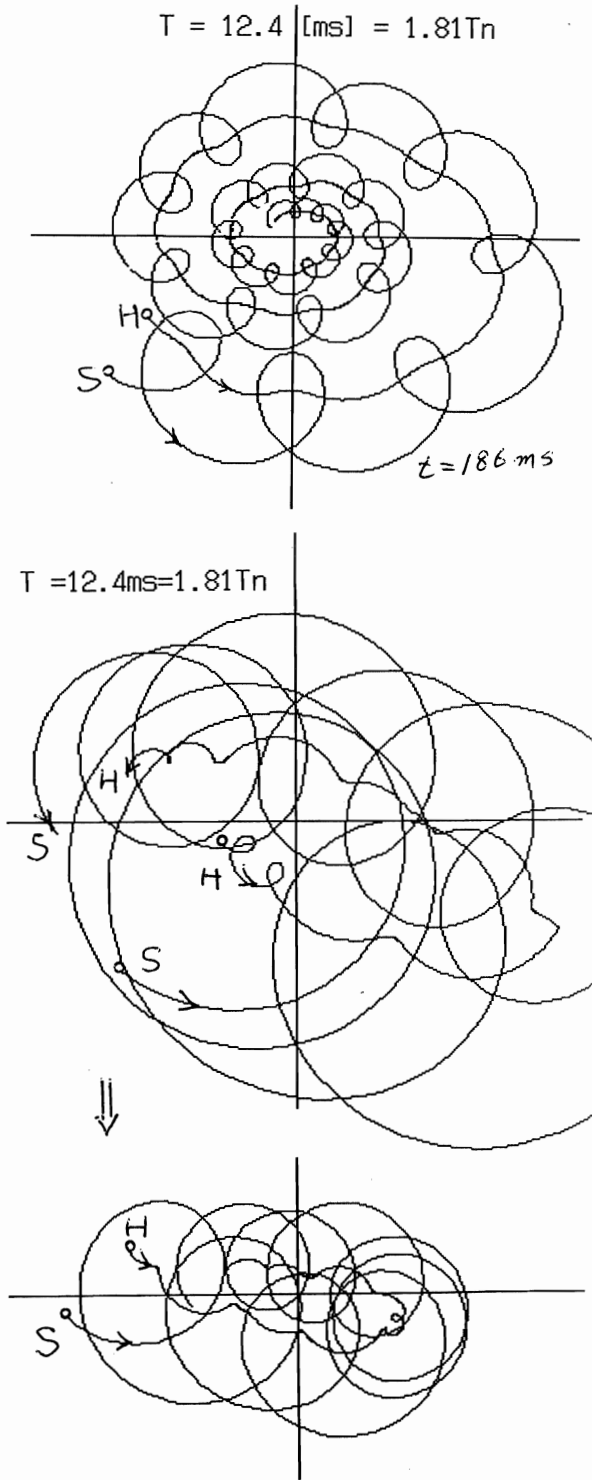


FIGURE 6 : $T = 2.27 \times T_n$ Case

FIGURE 5 : Case of $T = 1.81 \times T_n$ with Two Different Initial Conditions